Impact of Nuclear Mass Uncertainties on the *r* Process

D. Martin,[1,2,*] A. Arcones,[1,2,†] W. Nazarewicz,[3,4,‡] and E. Olsen[5,§]
[1]*Institut für Kernphysik, Technische Universität Darmstadt, Schlossgartenstrasse 2, Darmstadt D-64289, Germany*
[2]*GSI Helmholtzzentrum für Schwerionenforschung GmbH, Planckstrasse 1, Darmstadt D-64291, Germany*
[3]*Department of Physics and Astronomy and FRIB Laboratory, Michigan State University, East Lansing, Michigan 48824, USA*
[4]*Institute of Theoretical Physics, Faculty of Physics, University of Warsaw, 02-093 Warsaw, Poland*
[5]*NSCL/FRIB Laboratory, Michigan State University, East Lansing, Michigan 48824, USA*
(Received 10 December 2015; published 25 March 2016)

Nuclear masses play a fundamental role in understanding how the heaviest elements in the Universe are created in the *r* process. We predict *r*-process nucleosynthesis yields using neutron capture and photodissociation rates that are based on the nuclear density functional theory. Using six Skyrme energy density functionals based on different optimization protocols, we determine for the first time systematic uncertainty bands—related to mass modeling—for *r*-process abundances in realistic astrophysical scenarios. We find that features of the underlying microphysics make an imprint on abundances especially in the vicinity of neutron shell closures: Abundance peaks and troughs are reflected in trends of neutron separation energy. Further advances in the nuclear theory and experiments, when linked to observations, will help in the understanding of astrophysical conditions in extreme *r*-process sites.

DOI: 10.1103/PhysRevLett.116.121101

Understanding the origin of elements in nature is one of the outstanding questions in science. Here, the synthesis of the heavy elements represents a difficult interdisciplinary challenge. Half of the heavy elements up to bismuth and all of the thorium and uranium in the Universe are produced by the rapid capture of neutrons in the *r* process [1]. This process requires high neutron densities and involves extreme neutron-rich nuclei not yet produced in the laboratory.

In recent years, much progress has been made toward solving this problem in both astrophysics and nuclear physics. In astrophysics, multidimensional hydrodynamic simulations including improved microphysics indicate that (i) neutrino-driven winds following core-collapse supernovae are not neutron-rich enough to produce heavy elements as suggested in [2] (see Ref. [3] for a review), (ii) a rare kind of core-collapse supernova triggered by magnetic fields leads to neutron-rich jets where the *r* process can occur [4–6], and (iii) neutron star mergers (as suggested in [7] and preliminarily studied in [8]) are excellent candidates for the synthesis of heavy elements [9–11] even if their contribution to the early Galaxy is still under discussion. Some studies show that neutron star mergers provide an important contribution to the Solar System *r* process, but this is not enough to explain the abundances in the oldest observed stars; see, e.g., [12–14]. In contrast, other models can explain the *r*-process abundances at all metallicities solely based on the neutron star merger scenario [15].

Experimentally, there has been impressive progress in approaching *r*-process nuclei; see [16–21], and references quoted therein. New-generation radioactive ion beam facilities [22–24] will be able to reach a range of nuclei never possible before, including the neutron-rich frontier of the nuclear landscape. Theoretically, there have been major advances in both nuclear modeling and astrophysical simulations, greatly facilitated by high-performance computing [25–34]. When it comes to the nuclear input for the *r* process, one relies on global predictions of nuclear properties [35–38]. A microscopic tool that is well suited to provide quantified microphysics anywhere on the nuclear chart is the nuclear density functional theory (DFT) [39] based on a realistic energy density functional (EDF) representing the density-dependent effective nuclear interaction. This approach is capable of predicting a variety of observables needed and is able to assess the uncertainties on those observables, both statistical and systematic [40,41]. Such a capability is essential in the context of making extrapolations into the regions where experiments are impossible [41–44].

Objectives.—In this study, we present the impact of systematic uncertainties on nuclear masses for the two most promising astrophysical *r*-process scenarios: neutron star mergers [9] and jetlike supernovae [4]. The systematic (model) uncertainties are estimated by considering several EDFs optimized to experimental data. The corresponding systematic error thus represents the root-mean-squared spread of predictions of different EDF parametrizations obtained by means of diverse fitting protocols. In the absence of the exact reference model, such an intermodel deviation should be viewed as a rough approximation to the systematic error. A similar strategy was employed to estimate the position of neutron and proton drip lines [42,45], to study the landscape of two-proton radioactivity [46], and to assess neutron-skin uncertainties [44]. This approach is complementary to varying individual masses within some assumed error bars [37,47,48] or considering mass models and mass formulas based on vastly different physical approaches [35,49].

Method.—Nucleosynthesis calculations are performed within a complete nuclear reaction network (see Ref. [50] and references therein). The masses of even-even nuclei were computed in Ref. [42] for six different Skyrme EDFs: SkM* [51], SkP [52], SLy4 [53], SV-min [54], UNEDF0 [55], and UNEDF1 [56]. (For the corresponding mass tables, see Ref. [57].) The masses of odd-A and odd-odd isotopes were obtained by adding computed average pairing gaps to the binding energy of the corresponding zero-quasiparticle vacuum obtained by averaging binding energies of even-even neighbors; see Supplemental Material of Ref. [42].

For each EDF model, we compute Maxwellian-averaged (n,γ) reaction rates in the framework of the statistical model [58] using the TALYS code [59] with standard input (apart from the masses). This model relies on the assumption of a thermodynamic equilibrium in combination with compound nucleus reactions for excited states. Photodissociation rates are determined by a detailed balance with partition functions that are consistently obtained from the statistical model. In the reaction network, all (γ,n) and (n,γ) rates are replaced by new ones based on individual EDF parametrizations. Beta decay and fission rates have been taken at default values; those will be addressed in forthcoming work. Beta decay rates are not expected to dramatically change when varying mass models as compared to photodissociation reaction rates, which depend exponentially on the separation energy. Moreover, the impact of beta decays on the abundances have been shown to be moderate [16,17,19,60,61]. For fission we use the same input as in Refs. [9,50] that is based on Refs. [62–64]. Therefore, fission barriers and yield distributions are not consistent with the underlying mass model. Note, however, that the majority of models of fission yields currently used in r-process simulations are based on a simplistic barrier penetration approach that employs a notion of the static fission barrier. As this approach ignores collective dynamics, current fission models are prone to errors that exceed uncertainties related to the assumed input (mass models); see the discussion in Ref. [65]. In neutron star mergers, fission can have a big impact on the abundances around the second peak [9,36,61,66]. Consequently, in the results presented below, the impact of mass uncertainties on this region should be taken with caution, while for the third r-process peak our conclusions are robust.

Results.—The neutron capture and photodissociation rates based on Skyrme-DFT masses [42] have been used to calculate r-process abundances in neutron star mergers and jetlike supernovae. The various EDFs lead to different abundances; this variation is expected given their different optimization schemes. Therefore, when the six mass sets are considered, we obtain a systematic uncertainty band for the r-process abundances as shown in Fig. 1.

The Solar System r-process abundances do not always lie within the uncertainty band. This indicates that

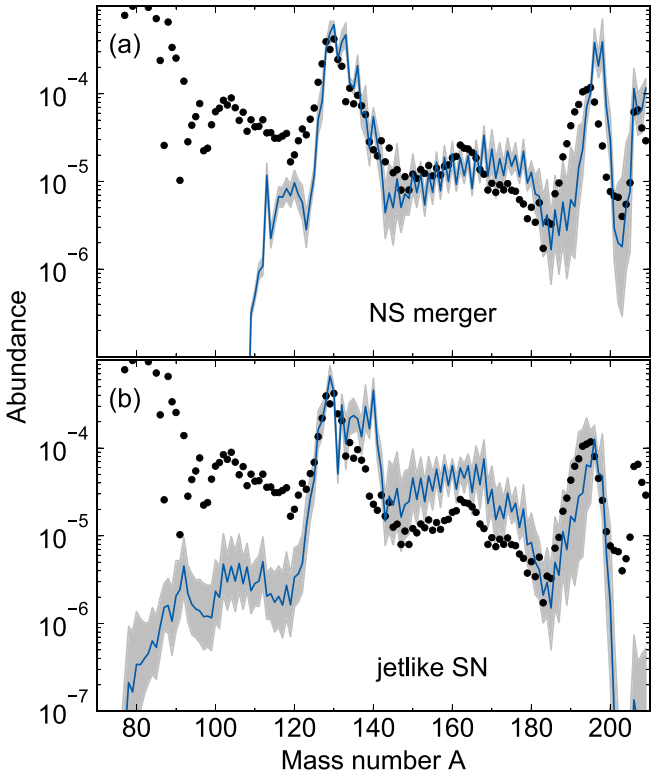

FIG. 1. Predicted abundance distributions for neutron star mergers (top) and jetlike supernovae (bottom). Dots indicate the Solar System r-process abundances. The systematic uncertainties (gray bands) are due to variations of the masses predicted in the six Skyrme-DFT models of Ref. [42]. The mean predicted abundances are marked by the solid line.

improvements in nuclear physics and astrophysical inputs are still necessary. However, important hints for future developments are offered by inspecting our uncertainty estimates. For example, the uncertainty band is not uniform but strongly depends on the mass number. This is in contrast to the sensitivity studies summarized in Ref. [48]. Therein, they find a broad and homogeneous uncertainty band for all mass numbers as a consequence of randomly varying individual masses within the same range. In our work, mass variations are correlated through the microscopic framework employed. The mass dependence can be seen in the abundances for neutron star mergers in Fig. 1(a), where the uncertainty band is narrow for the second r-process peak ($A \sim 130$) and broadens up before the third peak ($A \sim 195$). The second peak gets its major contribution from fission [9,61]. Since in this pilot study we are using the same fission barrier and yield distribution data for the six mass sets, only small variations are expected in this region. In contrast, the evolution of nuclear masses as a function of the neutron number critically impacts the abundances around shell closures when nuclei change character from deformed to spherical and back to deformed again. This occurs around neutron magic numbers where the abundance peaks form, thus leading to a broad

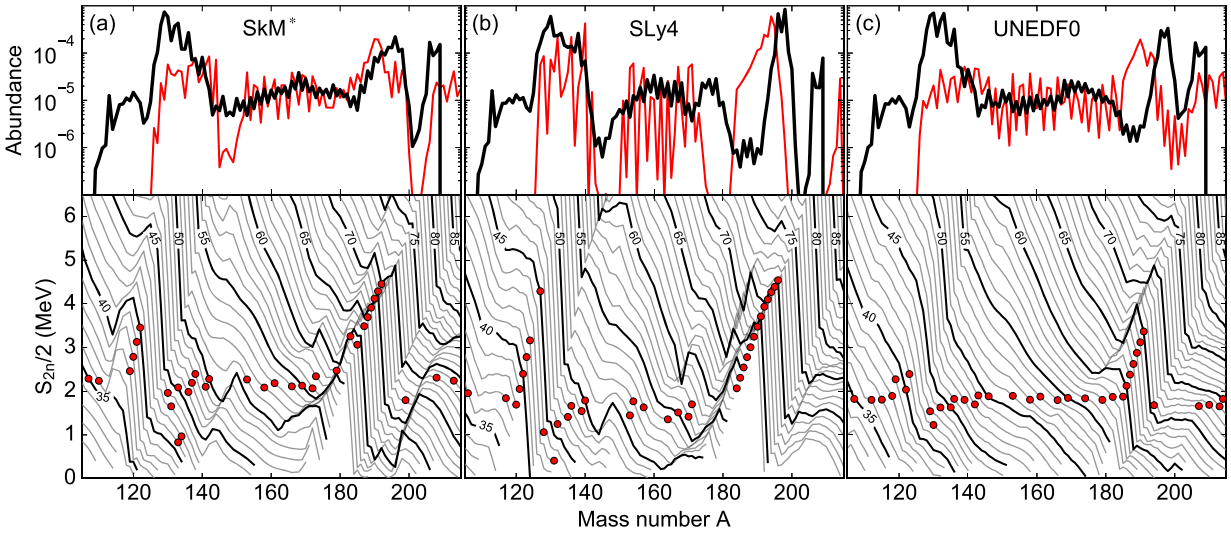

FIG. 2. Predictions of the SkM*, SLy4, and UNEDF0 models. Bottom: (Half of the) two-neutron separation energies along different isotopic chains (gray lines); every fifth isotope chain is plotted with black lines. The red dots correspond to the freeze-out abundances, i.e., the r-process path before matter starts to decay to stability. A few dots around $A \sim 135$ lie below the separation energy that is expected from $(n,\gamma) - (\gamma,n)$ equilibrium. Here, fission of nuclei with $A > 240$ populates regions beyond the r-process path. Top: The freeze-out (thin red lines) and final (thick black lines) abundances for a neutron star merger scenario.

uncertainty band. Since fission plays a minor role for jetlike supernovae in Fig. 1(b), the uncertainty band is broader than in the case of neutron star mergers before and after the second r-process peak.

In order to better understand the impact of nuclear masses on the predicted abundances, in Fig. 2 (bottom panels) we analyze the trend of two-neutron separation energies S_{2n} for the SkM*, SLy4, and UNEDF0 models. The red dots indicate the r-process path at freeze-out, i.e., the mass number with the highest abundance for every isotopic chain. At r-process freeze-out, most of the neutrons are consumed, and neutron-rich material starts to decay to stability. The abundances at freeze-out are marked by thin red lines in the upper panels, while the final abundances, following beta decays back to the valley of stability, are indicated by thick black lines.

The most remarkable features are the rapid variations of separation energies of neutron-rich nuclei at $A \approx 120$–140 and $A \approx 180$–200 associated with the neutron magic numbers $N = 82$ and 126, respectively. Moreover, one can identify the formation of peaks shown in the freeze-out abundances with the regions where matter accumulates (red dots). The third r-process peak at freeze-out is located at smaller mass numbers than in the final abundances, pointing to some important reactions occurring during the decay to stability. Beta decays keep the mass number constant or reduce it in the case of beta-delayed neutron emission (which can be significant as it increases the number of neutrons). This deviation indicates that the shift of the third peak is due to neutron captures [35,67]. Neutrons are thus critical in understanding both the evolution toward stability and the final abundances. In addition to the few leftover neutrons after freeze-out, there are also contributions from beta-delayed neutron emission and fission. In the case of neutron star mergers [61], there are many neutrons produced in fission, and this leads to a more pronounced shift of the third peak than in jetlike supernovae (Fig. 1).

The results shown in Fig. 2 were obtained using three EDFs developed using different optimization protocols. The functional SkM* [51] is the traditional Skyrme EDF fitted to binding energies and charge radii of selected spherical nuclei, spin-orbit splitting in ^{16}O, giant resonance energies in ^{208}Pb, and fission barriers. The functional SLy4 [53] was optimized with a focus on neutron-rich nuclei and neutron matter. In addition to properties of spherical nuclei, this functional was also constrained to basic properties of symmetric nuclear matter and the equation of state for pure neutron matter. Finally, a more recent model UNEDF0 [55] was carefully optimized to a large database including masses of spherical and deformed nuclei, charge radii of spherical nuclei, odd-even mass differences, and selected nuclear matter properties. These models have different performances when it comes to masses. The older models SkM* and SLy4 yield a large rms deviation from experiment, around and greater than 5 MeV. This can be attributed to an overemphasis on doubly magic nuclei during optimization as well as a fairly limited data set. As discussed in Ref. [55], the functional UNEDF0, with its rms deviation of 1.45 MeV, is probably within a few hundreds of keV of a globally optimal mass fit within the Skyrme EDF parameter space. To put things in perspective, we note that the best overall agreement with experimental masses, obtained with the Skyrme EDF, is around 600 keV [68]. However, this

excellent result was obtained at a price of several phenomenological corrections on top of the original Skyrme-DFT model.

The parametrization SkM* is the one that leads to the smallest shift of the third peak from freeze-out to final abundances. For SLy4, the third peak is strongly shifted compared to SkM*, and there is a big trough in abundances before it. The trough corresponds to the region without dots in the lower panel of Fig. 2(b) ($A \sim 180$). The origin of this trough is the nonmonotonic behavior of the separation energy [35,69] predicted in this model. In order to illustrate the behavior of the freeze-out abundances before $N = 126$, the left panel of Fig. 3 shows S_{2n} in SLy4 and UNEDF0 in the region where the third r-process peak forms. Far from stability, the r-process path stays at an almost constant neutron separation energy during the $(n,\gamma) - (\gamma,n)$ equilibrium. This value is marked in Figs. 3(a) and 3(b) by the dashed line at a representative value of $S_{2n}/2 = 1.5$ MeV. Note that the explanation here is valid for any $(n,\gamma) - (\gamma,n)$ equilibrium, in general, but inspired by the values found in Fig. 2. When matter approaches this limit, it stays there until a beta decay occurs. Afterwards, more neutron captures are possible until the separation energy reaches this limit again. Figure 3(a) shows that for SLy4 the nonmonotonic behavior of S_{2n} leads to a long sequence of neutron captures at a fixed Z value; hence, it results in a trough in the abundances versus mass number. In the case of UNEDF0, on the other hand, after a beta decay, the $(n,\gamma) - (\gamma,n)$-equilibrium S_n is reached again after only a few neutron captures. The nonmonotonic behavior of neutron separation energies can be traced back to structural changes due to rapid shape transitions from prolate to spherical to oblate. While the global deformation patterns predicted by various EDFs are fairly similar [42], the subtle details of shape transitions are predicted differently. This is illustrated in Figs. 3(c) and 3(d) for SLy4 and UNEDF0, respectively.

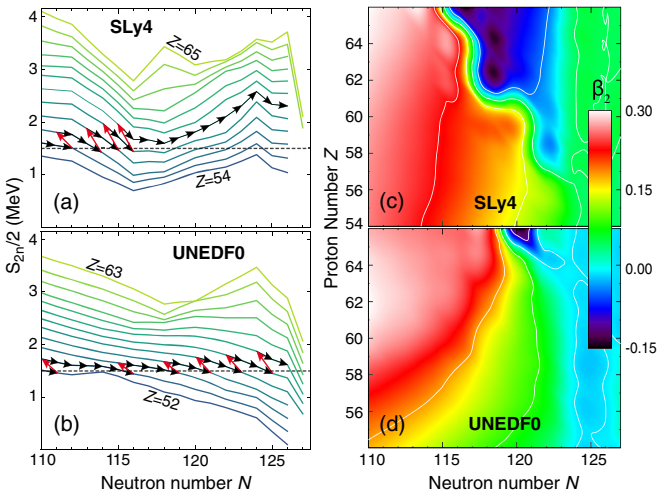

FIG. 3. Left: Half of the two-neutron separation energies predicted by the models SLy4 (a) and UNEDF0 (b) versus the neutron number in the region where the third r-process peak forms. The dashed line marks the approximate r-process path during $(n,\gamma) - (\gamma,n)$ equilibrium ($S_{2n}/2 = 1.5$ MeV). Black arrows indicate neutron captures; red arrows mark beta decays along the path. Right: The corresponding quadrupole deformations β_2 for SLy4 (c) and UNEDF0 (d).

The functional UNEDF0, informed by experimental masses in spherical and deformed nuclei, exhibits a smoother evolution of S_{2n} versus A than other functionals considered. In fact, it is so much less steep for $N = 82$ that the shell closure is quenched for very neutron-rich nuclei with $Z \leq 40$; see Fig. 2(c). This results in the lack of the second peak in the freeze-out abundances. However, as discussed above, the second peak in the final abundances has its origin in fission.

The freeze-out abundances and the evolution toward stability to produce the final abundances depend on astrophysical conditions. For the jetlike supernova trajectory, the freeze-out path is closer to stability (i.e., at higher neutron separation energies) and there are less neutrons available during the decay because of the reduced effect of fission. The features that we have explained before for the neutron star merger affect the jetlike supernova abundance differently. Therefore, reducing uncertainties in the nuclear physics input should enable us to use observations to constrain and understand the astrophysical conditions related to the r-process site.

Conclusions.—In summary, we have shown that detailed features of nuclear mass evolution toward the neutron drip line are critical to understand both the abundances and the origin of heavy elements in the r process. Of utmost importance are the regions around magic numbers where separation energies vary rapidly due to spherical shell closures and shape changes. The systematic uncertainty band obtained within the deformed Skyrme-DFT approach exhibits significant variations with particle number. It is encouraging, however, that in certain mass regions the model error is fairly small; i.e., the intermodel consistency of our results can be high. The regions characterized by the broad uncertainty bands in Fig. 1 are indicative of model differences far from stability, where the theory relies on (sometimes extreme) extrapolations. To reduce the uncertainties, the development of nuclear EDFs of spectroscopic quality, constrained by data on the most neutron-rich nuclei reachable in experiments, is needed. In this respect, the r-process abundance predictions presented in this work aim at assessing the current status of theoretical mass modeling at the limits of nuclear binding and also provide a useful benchmark for future improvements. In the next step, we intend to improve other microphysics input, such as fission yields and beta decay rates, as well as to explore additional astrophysical environments.

It would be interesting to evaluate systematic uncertainty bands for other microscopic mass models based on effective interactions (or EDFs). In this context, we note that

mass predictions performed within the covariant DFT [45] have provided separation-energy uncertainties remarkably similar to those from Skyrme-DFT [42]. Finally, we wish to emphasize that our methodology, based on model-based extrapolations (hence, considering correlations between predicted masses) is complementary to and different from sensitivity studies based on individual mass variations (see, e.g., [48]) resulting in a homogeneous uncertainty band for all masses.

We thank Julia Bliss for useful discussions about the nucleosynthesis. This work was supported by Helmholtz-University Young Investigator Grant No. VH-NG-825; by the BMBF under Grant No. 05P15RDFN1; by the U.S. Department of Energy, Office of Science under Awards No. DE-SC0013365 (Michigan State University), No. DE-SC0008511 (NUCLEI SciDAC-3 Collaboration), and No. DE-NA0002574 (the Stewardship Science Academic Alliances program).

*dirk.martin@physik.tu-darmstadt.de
†almudena.arcones@physik.tu-darmstadt.de
‡witek@frib.msu.edu
§olsene@nscl.msu.edu

[1] M. Arnould, S. Goriely, and K. Takahashi, Phys. Rep. **450**, 97 (2007).
[2] S. E. Woosley, J. R. Wilson, G. J. Mathews, R. D. Hoffman, and B. S. Meyer, Astrophys. J. **433**, 229 (1994).
[3] A. Arcones and F.-K. Thielemann, J. Phys. G **40**, 013201 (2013).
[4] C. Winteler, R. Käppeli, A. Perego, A. Arcones, N. Vasset, N. Nishimura, M. Liebendörfer, and F.-K. Thielemann, Astrophys. J. Lett. **750**, L22 (2012).
[5] P. Mösta, S. Richers, C. D. Ott, R. Haas, A. L. Piro, K. Boydstun, E. Abdikamalov, C. Reisswig, and E. Schnetter, Astrophys. J. Lett. **785**, L29 (2014).
[6] N. Nishimura, T. Takiwaki, and F.-K. Thielemann, Astrophys. J. **810**, 109 (2015).
[7] J. M. Lattimer and D. N. Schramm, Astrophys. J. Lett. **192**, L145 (1974).
[8] C. Freiburghaus, S. Rosswog, and F.-K. Thielemann, Astrophys. J. Lett. **525**, L121 (1999).
[9] O. Korobkin, S. Rosswog, A. Arcones, and C. Winteler, Mon. Not. R. Astron. Soc. **426**, 1940 (2012).
[10] S. Goriely, A. Bauswein, and H.-T. Janka, Astrophys. J. Lett. **738**, L32 (2011).
[11] S. Wanajo, Y. Sekiguchi, N. Nishimura, K. Kiuchi, K. Kyutoku, and M. Shibata, Astrophys. J. Lett. **789**, L39 (2014).
[12] F. Matteucci, D. Romano, A. Arcones, O. Korobkin, and S. Rosswog, Mon. Not. R. Astron. Soc. **438**, 2177 (2014).
[13] B. Wehmeyer, M. Pignatari, and F.-K. Thielemann, Mon. Not. R. Astron. Soc. **452**, 1970 (2015).
[14] S. Shen, R. J. Cooke, E. Ramirez-Ruiz, P. Madau, L. Mayer, and J. Guedes, Astrophys. J. **807**, 115 (2015).
[15] Y. Ishimaru, S. Wanajo, and N. Prantzos, Astrophys. J. Lett. **804**, L35 (2015).
[16] P. Hosmer *et al.*, Phys. Rev. C **82**, 025806 (2010).
[17] M. Madurga *et al.*, Phys. Rev. Lett. **109**, 112501 (2012).
[18] H. Watanabe *et al.*, Phys. Rev. Lett. **111**, 152501 (2013).
[19] G. Lorusso *et al.*, Phys. Rev. Lett. **114**, 192501 (2015).
[20] D. Atanasov *et al.*, Phys. Rev. Lett. **115**, 232501 (2015).
[21] C. Mazzocchi *et al.*, Phys. Rev. C **92**, 054317 (2015).
[22] *Nuclear Physics: Exploring the Heart of Matter. Report of the Committee on the Assessment of and Outlook for Nuclear Physics* (National Academies Press, Washington, DC, 2012).
[23] NuPECC long range plan report, 2010.
[24] NSAC long range plan report, 2015.
[25] A. B. Balantekin *et al.*, Mod. Phys. Lett. A **29**, 1430010 (2014).
[26] S. Bogner *et al.*, Comput. Phys. Commun. **184**, 2235 (2013).
[27] S. Binder, J. Langhammer, A. Calci, and R. Roth, Phys. Lett. B **736**, 119 (2014).
[28] T. A. Lähde, E. Epelbaum, H. Krebs, D. Lee, U.-G. Meißner, and G. Rupak, Phys. Lett. B **732**, 110 (2014).
[29] G. Hagen *et al.*, Nat. Phys. **12**, 186 (2016).
[30] K. Hebeler, J. D. Holt, J. Menéndez, and A. Schwenk, Annu. Rev. Nucl. Part. Sci. **65**, 457 (2015).
[31] H.-T. Janka, Annu. Rev. Nucl. Part. Sci. **62**, 407 (2012).
[32] S. M. Couch and C. D. Ott, Astrophys. J. **799**, 5 (2015).
[33] C. Palenzuela, S. L. Liebling, D. Neilsen, L. Lehner, O. L. Caballero, E. O'Connor, and M. Anderson, Phys. Rev. D **92**, 044045 (2015).
[34] P. Mösta, C. D. Ott, D. Radice, L. F. Roberts, E. Schnetter, and R. Haas, Nature (London) **528**, 376 (2015).
[35] A. Arcones and G. Martínez-Pinedo, Phys. Rev. C **83**, 045809 (2011).
[36] S. Goriely, J.-L. Sida, J.-F. Lemaitre, S. Panebianco, N. Dubray, S. Hilaire, A. Bauswein, and H.-T. Janka, Phys. Rev. Lett. **111**, 242502 (2013).
[37] M. R. Mumpower, R. Surman, D.-L. Fang, M. Beard, P. Möller, T. Kawano, and A. Aprahamian, Phys. Rev. C **92**, 035807 (2015).
[38] J. J. Mendoza-Temis, M.-R. Wu, K. Langanke, G. Martínez-Pinedo, A. Bauswein, and H.-T. Janka, Phys. Rev. C **92**, 055805 (2015).
[39] M. Bender, P.-H. Heenen, and P.-G. Reinhard, Rev. Mod. Phys. **75**, 121 (2003).
[40] J. Dobaczewski, W. Nazarewicz, and P.-G. Reinhard, J. Phys. G **41**, 074001 (2014).
[41] J. D. McDonnell, N. Schunck, D. Higdon, J. Sarich, S. M. Wild, and W. Nazarewicz, Phys. Rev. Lett. **114**, 122501 (2015).
[42] J. Erler, N. Birge, M. Kortelainen, W. Nazarewicz, E. Olsen, A. M. Perhac, and M. Stoitsov, Nature (London) **486**, 509 (2012).
[43] Y. Gao, J. Dobaczewski, M. Kortelainen, J. Toivanen, and D. Tarpanov, Phys. Rev. C **87**, 034324 (2013).
[44] M. Kortelainen, J. Erler, W. Nazarewicz, N. Birge, Y. Gao, and E. Olsen, Phys. Rev. C **88**, 031305 (2013).
[45] A. V. Afanasjev, S. E. Agbemava, D. Ray, and P. Ring, Phys. Lett. B **726**, 680 (2013).
[46] E. Olsen, M. Pfützner, N. Birge, M. Brown, W. Nazarewicz, and A. Perhac, Phys. Rev. Lett. **110**, 222501 (2013); **111**, 139903(E) (2013).
[47] M. Mumpower, R. Surman, D. L. Fang, M. Beard, and A. Aprahamian, J. Phys. G **42**, 034027 (2015).

[48] M. Mumpower, R. Surman, G. McLaughlin, and A. Aprahamianan, Prog. Part. Nucl. Phys. **86**, 86 (2016).
[49] K. Farouqi, K.-L. Kratz, L. I. Mashonkina, B. Pfeiffer, J. J. Cowan, F.-K. Thielemann, and J. W. Truran, Astrophys. J. Lett. **694**, L49 (2009).
[50] D. Martin, A. Perego, A. Arcones, F.-K. Thielemann, O. Korobkin, and S. Rosswog, Astrophys. J. **813**, 2 (2015).
[51] J. Bartel, P. Quentin, M. Brack, C. Guet, and H.-B. Håkansson, Nucl. Phys. **A386**, 79 (1982).
[52] J. Dobaczewski, H. Flocard, and J. Treiner, Nucl. Phys. **A422**, 103 (1984).
[53] E. Chabanat, P. Bonche, P. Haensel, J. Meyer, and R. Schaeffer, Nucl. Phys. **A635**, 231 (1998).
[54] P. Klüpfel, P.-G. Reinhard, T. J. Bürvenich, and J. A. Maruhn, Phys. Rev. C **79**, 034310 (2009).
[55] M. Kortelainen, T. Lesinski, J. Moré, W. Nazarewicz, J. Sarich, N. Schunck, M. V. Stoitsov, and S. Wild, Phys. Rev. C **82**, 024313 (2010).
[56] M. Kortelainen, J. McDonnell, W. Nazarewicz, P.-G. Reinhard, J. Sarich, N. Schunck, M. V. Stoitsov, and S. M. Wild, Phys. Rev. C **85**, 024304 (2012).
[57] http://massexplorer.frib.msu.edu.
[58] J. A. Holmes, S. E. Woosley, W. A. Fowler, and B. A. Zimmerman, At. Data Nucl. Data Tables **18**, 305 (1976).
[59] A. J. Koning, S. Hilaire, and S. Goriely, TALYS 1.6 user manual, http://www.talys.eu/fileadmin/talys/user/docs/talys1.6.pdf.
[60] N. Nishimura, T. Kajino, G. J. Mathews, S. Nishimura, and T. Suzuki, Phys. Rev. C **85**, 048801 (2012).
[61] M. Eichler, A. Arcones, A. Kelic, O. Korobkin, K. Langanke, T. Marketin, G. Martinez-Pinedo, I. V. Panov, T. Rauscher, S. Rosswog, C. Winteler, N. T. Zinner, and F.-K. Thielemann, Astrophys. J. **808**, 30 (2015).
[62] I. V. Panov, C. Freiburghaus, and F.-K. Thielemann, Nucl. Phys. **A688**, 587 (2001).
[63] I. V. Panov, E. Kolbe, B. Pfeiffer, T. Rauscher, K.-L. Kratz, and F.-K. Thielemann, Nucl. Phys. **A747**, 633 (2005).
[64] I. V. Panov, I. Y. Korneev, T. Rauscher, G. Martínez-Pinedo, A. Kelić-Heil, N. T. Zinner, and F.-K. Thielemann, Astron. Astrophys. **513**, A61 (2010).
[65] J. Sadhukhan, W. Nazarewicz, and N. Schunck, Phys. Rev. C **93**, 011304 (2016).
[66] S. Shibagaki, T. Kajino, G. J. Mathews, S. Chiba, S. Nishimura, and G. Lorusso, Astrophys. J. **816**, 79 (2016).
[67] R. Surman and J. Engel, Phys. Rev. C **64**, 035801 (2001).
[68] S. Goriely, N. Chamel, and J. M. Pearson, Phys. Rev. C **88**, 024308 (2013).
[69] A. Arcones and G. F. Bertsch, Phys. Rev. Lett. **108**, 151101 (2012).